

Autorização concedida ao Repositório Institucional da Universidade de Brasília (RIUnB) pelo Professor Ugo Silva Dias, em 19 de dezembro de 2018, para disponibilizar o trabalho, gratuitamente, para fins de leitura, impressão e/ou download, a título de divulgação da obra.

## REFERÊNCIA

ILLI, Elmehdi et al. On the secrecy performance of mixed RF/UOW communication system. In: IEEE GLOBAL COMMUNICATIONS CONFERENCE, 2018; IEEE GLOBECOMWORKSHOP ON TRUSTED COMMUNICATIONS WITH PHYSICAL LAYER SECURITY, 6., 2018, Abu Dhabi, UAE.

# On the Secrecy Performance of Mixed RF/UOW Communication System

Elmehdi Illi<sup>1</sup>, Faissal El Bouanani<sup>1</sup>, Daniel Benevides da Costa<sup>2</sup>, Fouad Ayoub<sup>3</sup>, and Ugo S. Dias<sup>4</sup>

<sup>1</sup>ENSIAS, Mohammed V University in Rabat, Morocco

<sup>2</sup>Federal University of Ceará (UFC), Sobral, Brazil

<sup>3</sup>CRMEF Kenitra, Morocco

<sup>4</sup>University of Brasília, DF, Brazil

Emails: {elmehdi.illi, f.elbouanani}@um5s.net.ma, danielbcosta@ieee.org, ayoub@crmekf.ma, ugodias@ieee.org

**Abstract**—In this paper, the secrecy performance of a dual-hop mixed radio-frequency/underwater optical wireless communication (RF/UOWC) system is investigated. The considered system consists of one single antenna source node ( $S$ ) communicating with one destination node ( $D$ ), considered as the legitimate receiver, through the help of one amplify-and-forward (AF) relay node  $R$  equipped with multiple antennas for reception. Specifically, the relay receives the incoming signal from  $S$  via an RF link, applies maximal-ratio combining (MRC) technique, amplifies the output combined signal with a fixed gain, and then forwards it to  $D$  via an UOWC link. The transmission protocol is performed under the eavesdroppers' attempt to overhear the RF link (i.e.,  $S-R$ ). We derive an exact closed-form expression for the secrecy intercept probability (IP) in terms of the Fox's  $H$ -function, or in terms of the Meijer's  $G$ -function as a particular case. The derived secrecy performance metric is evaluated in terms of various channel and system parameters, and corroborated by Monte-Carlo simulation method. Our derived analytical formulas present an efficient tool to highlight the impact of some system and channel parameters on the secrecy performance, namely the number of relay antennas, number of eavesdropping nodes, relay gain, fading severity of RF links, and water turbulence severity of the UOWC link.

**Keywords**—Dual-hop relaying, performance analysis, physical layer security, radio-frequency link, underwater optical wireless communication link.

## I. INTRODUCTION

Along the last years, the scientific community has witnessed a notable increase of human activities in the underwater environments [1]. Underwater wireless communication technology has indeed gained great interest recently as it permits the realization of many potential applications, e.g., oil production and control, ecological monitoring, climate recording, and military surveillance [2]. Due to its limited bandwidth, neither the traditional acoustic nor radio-frequency (RF) technologies seem able to provide high-speed underwater communications [3]. Besides, the acoustic link suffers from serious communication delays. As a consequence, the implementation of real-time high-speed underwater applications through acoustic links remains a challenging objective to achieve [1]. By its turn, underwater optical wireless communication (UOWC) technology has also received considerable attention, as a promising key-enabling technology for large volume high-speed underwater communications [4]. While acoustic communication provides

very low data rate and serious communication delays, UOWC technology may offer a data rate up to tens of Gbps at moderate propagation distance (tens of meters) [3]. Additionally, high communication security, low latency, as well as low energy consumption make optical communication widely accepted as an appropriate communication solution in the underwater medium [4].

Despite all of these promising features, light propagation under water is highly corrupted by the turbulence phenomenon [5]. Turbulence is regarded as the event that makes water's refractive index change rapidly, due to the temperature and pressure inhomogeneities in the marine medium. Such effect is often caused by ocean currents, leading to sudden variations in the water pressure and temperature [2].

With this remarkably increasing demand towards deploying optical communication in marine environments, there has been an urgent need to make a comprehensive study in order to identify the attenuation effects of the underwater medium on light propagation [2]. Up to date, few works have modeled the UOWC channel's turbulence impairment. Most of the conducted studies were proposed based on the already existing terrestrial free-space optical (FSO) or indoor OWC link turbulence models [2]. In particular, the authors proposed in [6] the Lognormal turbulence model, mostly familiar with modeling terrestrial FSO links, to characterize irradiance fluctuation caused by water turbulence, by considering the similarity of underwater and atmospheric optical turbulence. However, due to the fact that underwater turbulence behavior is different from its atmospheric counterpart, Lognormal model appears to be inaccurate to represent this impairment in the marine medium [1]. In [5], a more accurate mixture Exponential-Lognormal turbulence model has been proposed in this matter to represent irradiance fluctuations. Nevertheless, this model shows its validity for specific values of scintillation index. The authors in [2] proposed the Exponential-Gamma UOWC turbulence model, which characterizes particularly, the vast majority of turbulence conditions in the marine medium (weak to strong), over both fresh and salty waters. Moreover, it is a more tractable analytical model compared to its Exponential/Lognormal counterpart, making it a widely universal and simple model to apply.

Dual-hop communication links have been proposed as a

fair solution for long-range communication links, as it provides wider network coverage as well as increased communication system's capacity [7]. In particular, with the limitations of terrestrial FSO links caused by atmospheric turbulence, mixed RF/FSO systems have been widely advocated in literature as an efficient solution to overcome optical channel's limitations. The overarching idea here is to place a relay node between the source and the destination ends, that is able to operate over both technologies (e.g., RF, FSO). The source node communicates through an RF link with the relay, which by its turn, converts the received signal to an optical light wave, and delivers it through an FSO link to the destination. Several investigations have been addressed in order to carry out mixed RF/FSO communication systems performance analysis. In [8], a performance analysis of a dual-hop mixed RF/FSO system was conducted, where both links are subject to Nakagami- $m$  and Gamma-Gamma fading channels, respectively. Likewise, a similar performance analysis to the previous one was performed in [9], by considering Málaga- $\mathcal{M}$  fading channel for the FSO link.

Physical layer security has been currently among critical discussed topics in wireless communication and information security [10]. Such interest becomes more attracting due to the broadcast nature of the wireless RF link, making it vulnerable to intrusion threats of potential eavesdropping devices, trying to overhear the legitimate communication channel [11]. In contrast with higher layers that view the security aspect as an implementation of cryptographic protocols, physical layer security paradigm, introduced by Wyner in [12], aims at exploiting the randomness property of the communication channel, alongside with channel coding, to realize perfectly secure communication [10]. Physical layer security has been widely addressed in the literature in several works. In [13], the secrecy performance of a multiple-input multiple-output (MIMO) system, subject to Nakagami- $m$  fading, was analyzed with the presence of a multiple-antenna eavesdropper. While in [14], the study dealt with the secrecy performance analysis in a multi-user and multi-eavesdropper cellular network. On the other hand, the secrecy analysis of FSO links was performed in [15], [16]. While the RF link is most likely vulnerable to eavesdropping attack due to its broadcast nature, FSO/UOWC links are more secure due to the highly directional light beam. As a consequence, the physical layer security of the mixed RF/FSO and RF/UOWC systems is of great consideration currently, since the RF hop can be easily attacked. Few works carried out the secrecy performance of mixed RF/FSO systems. For instance, [17] analyzed the secrecy performance in terms of average secrecy rate and secrecy outage probability of the mixed system proposed in [8], while [18], addressed the secrecy analysis for a multi-user multi-eavesdropper RF/FSO system. However, to the best of the authors' knowledge, the performance analysis of mixed RF/UOWC system, with appropriate underwater channel models has not been addressed yet.

The secrecy performance of mixed RF-optical links is still, an open topic, as there are few works that carried out the secrecy analysis of these systems. In the open literature, performances were analyzed exclusively for mixed RF/FSO systems. In this paper, in addition to considering a new mixed

configuration of an RF/UOWC system, we address the secrecy performance of this considered configuration with a multiple-antenna amplify-and-forward (AF) relay, and with the presence of multiple eavesdroppers. Channel turbulence parameters as well as the number of antennas, detection technique type, and the number of eavesdroppers are taken into account.

The main contributions of this paper are, at least, three-fold:

- Closed-form expressions for the statistical properties of the total end-to-end signal-to-noise ratio (SNR) of the legitimate link and the overall wiretap link are derived.
- The secrecy performance of the considered network is evaluated as a function of system and channel's parameters. Specifically, an exact closed-form expression for the intercept probability (IP), is derived assuming a fixed-gain relaying protocol.
- Our derived analytical results highlight the effect of key system parameters on the system's secrecy performance, namely the number of relay antennas, RF fading severity parameter of the legitimate and the wiretap links, eavesdroppers received power, and also water turbulence severity parameters of the UOWC link.

The remainder of this paper is organized as follows. Section II presents the adopted system and channel's models, while in Section III, statistical properties for the considered communication network are derived. In Section IV, an analytical expression for the intercept probability is derived. Some illustrative numerical examples are shown in Section V, followed by insightful discussions. Section VI concludes the paper with future directions.

## II. SYSTEM AND CHANNEL MODELS

We consider a dual-hop mixed communication system operating under mixed RF and UOWC technologies. In such scenario, the information signal is transmitted from the source node  $S$  (e.g., ground control station, boat), via an RF link, through an AF relay node  $R$  (e.g., floating buoy), that combines the received signal copies at its  $N_r$  receive antennas using MRC technique. After amplifying the combined signal with a fixed gain, the relay forwards it to the legitimate underwater destination node  $D$  (e.g., submarine) via an UOWC link. The communication is performed in the presence of multiple eavesdroppers attackers attempting to overhear the RF side of the communication link.

### A. Source ( $S$ )–Relay ( $R$ ) hop

In this paper, the signal envelope of the  $S - R$  link is modeled by a Nakagami- $m$  flat fading model. As a consequence, the SNR  $(\gamma_i)_{i=1,\dots,N_r}$  received at  $i$ th antenna  $A_i$  of  $R$  is Gamma distributed with probability density function (PDF) given by [19]

$$f_{\gamma_i}(z) = \sigma_i^{m_i} \frac{z^{m_i-1}}{\Gamma(m_i)} \exp(-\sigma_i z), z > 0, \quad (1)$$

where  $\sigma_i = \frac{m_i}{\bar{\gamma}_i}$ , and  $m_i$  and  $\bar{\gamma}_i$  denote the Nakagami- $m$  fading parameter and the average SNR of the  $S-A_i$  link, respectively. In what follows, we suppose the case of independent and identically distributed (i.i.d) diversity branches, that is  $m_i = m$  and  $\bar{\gamma}_i = \bar{\gamma}$ .

The relay node combines the received signal from  $S$  by using its  $N_r$  antennas through MRC technique. The total SNR  $\gamma_{SR}$  at the output of the MRC combiner can be expressed as

$$\gamma_{SR} = \sum_{i=1}^{N_r} \gamma_i. \quad (2)$$

Furthermore, the PDF and the cumulative distribution function (CDF) of the SNR  $\gamma_{SR}$ , are given by [20]

$$f_{\gamma_{SR}}(z) = \frac{\sigma^{mN_r}}{\Gamma(mN_r)} z^{mN_r-1} \exp(-\sigma z), \quad (3)$$

$$F_{\gamma_{SR}}(z) = \frac{\gamma_{inc}(mN_r, \sigma z)}{\Gamma(mN_r)}, \quad (4)$$

where  $\sigma = \frac{m}{\bar{\gamma}}$ , and  $\gamma_{inc}(\cdot, \cdot)$  and  $\Gamma(\cdot)$  denote the lower incomplete Gamma function [21, Eq. (8.350.1)] and the Gamma function [21, Eq. (8.310.1)], respectively.

### B. Source ( $S$ )–Eavesdropper ( $E$ ) hop

The wiretap link is composed by  $L$  eavesdroppers ( $E_i$ ) $_{1 \leq i \leq L}$ . Similarly, the links  $S-E_i$  are supposed to undergo i.i.d Nakagami- $m$  fading with PDF given by

$$f_{\gamma_{SE_i}}(z) = \sigma_e^{m_e} \frac{z^{m_e-1}}{\Gamma(m_e)} \exp(-\sigma_e z), \quad (5)$$

where  $\sigma_e = \frac{m_e}{\bar{\gamma}_e}$ , and  $m_e$  and  $\bar{\gamma}_e$  denote the Nakagami- $m$  fading parameter and the average SNR of the wiretap link between  $S$  and the eavesdropper node  $E_i$ , respectively.

The CDF of the  $S-E_i$  link between the source node and an eavesdropper  $E_i$  among the  $L$  eavesdroppers is given by

$$F_{\gamma_{SE_i}}(t) = \frac{\gamma_{inc}(m_e, \sigma_e t)}{\Gamma(m_e)}. \quad (6)$$

### C. Relay ( $R$ )–Destination ( $D$ ) hop

The  $R-D$  hop is an UOWC link, modeled by the mixture Exponential-Gamma model, where the PDF of the received light irradiance  $I_{RD}$  is given by [2]

$$f_{I_{RD}}(I) = \frac{\omega}{\lambda} \exp\left(-\frac{I}{\lambda}\right) + (1-\omega) I^{\alpha-1} \frac{\exp\left(-\frac{I}{\beta}\right)}{\beta^\alpha \Gamma(\alpha)}, I > 0, \quad (7)$$

where  $\omega$  denotes the mixture weight factor, such that  $\omega \in [0, 1]$ ,  $\alpha$  and  $\beta$  represent Gamma distribution's shape and scale parameters, respectively, and  $\lambda$  accounts for the Exponential distribution's mean.

The relationship between the irradiance and the SNR can be expressed as [7]

$$\gamma_{RD} = \frac{(\eta I_{RD})^r}{N_0}, \quad (8)$$

where  $\eta$  denotes the photodetector efficiency,  $r$  is a detection technique-dependent parameter (e.g.,  $r = 1$  refers to coherent detection, while  $r = 2$  for Intensity Modulation and Direct Detection (IM/DD) technique), and  $N_0$  denotes additive white Gaussian noise's (AWGN) power spectral density.

By applying the Jacobi transform on the PDF of  $I_{RD}$  expressed in (7), and by doing some algebraic manipulations, we obtain the PDF of the SNR  $\gamma_{RD}$  given by

$$f_{\gamma_{RD}}(z) = \frac{\omega}{r} \frac{\kappa}{\lambda} z^{\frac{1}{r}-1} \exp\left(-\frac{\kappa}{\lambda} z^{\frac{1}{r}}\right) + \frac{(1-\omega)}{r\Gamma(\alpha)} \left(\frac{\kappa}{\beta}\right)^\alpha z^{\frac{\alpha}{r}-1} \exp\left(-\frac{\kappa}{\beta} z^{\frac{1}{r}}\right), \quad (9)$$

where  $\kappa = \frac{\mathbb{E}[I]}{\mu_r^{\frac{1}{r}}}$ ,  $\mathbb{E}[I]$  denotes the average value of the received light irradiance defined as

$$\mathbb{E}[I] = \omega\lambda + (1-\omega)\alpha\beta, \quad (10)$$

and  $\mu_r$  stands for the average electrical SNR given by

$$\mu_r = \frac{\eta_e^r}{N_0} \mathbb{E}[I]. \quad (11)$$

## III. STATISTICAL PROPERTIES OF THE END-TO-END

In this section, a closed-form expression for the CDF of the total end-to-end SNR of the considered mixed RF/UOWC system is presented. Since the relay node amplifies the incoming signal by a fixed gain, the total end-to-end SNR at  $D$  can be expressed as [7], [22]

$$\gamma_{eq} = \frac{\gamma_{SR}\gamma_{RD}}{\gamma_{RD} + C}, \quad (12)$$

where  $C$  denotes a fixed-gain amplifying constant.

**Proposition 1.** The CDF of the total SNR  $\gamma_{eq}$  is given by

$$F_{\gamma_{eq}}(t) = 1 - \frac{e^{-\sigma t}}{r} \sum_{l=0}^{mN_r-1} \sum_{j=0}^l \frac{(\sigma t)^{l-j}}{j!(l-j)!} \times \left[ \omega V(\alpha, \beta) + \frac{(1-\omega)}{\Gamma(\alpha)} V(1, \lambda) \right], \quad (13)$$

where

$$V(x, y) = H_{0,2}^{2,0} \left( \epsilon(y) \left| \begin{matrix} -; - \\ (x, 1), (j, \frac{1}{r}) \end{matrix} ; - \right. \right) \quad (14)$$

$\epsilon(y) = \frac{\Delta}{y} t^{\frac{1}{r}}$ ,  $\Delta = \kappa(\sigma C)^{\frac{1}{r}}$ , and  $H_{p,q}^{m,n} \left( z \left| \begin{matrix} (a_i, A_i)_{i=1:p} \\ (b_k, B_k)_{k=1:q} \end{matrix} \right. \right)$ ,  $p \geq n$ , and  $q \geq m$ , is the Fox's  $H$ -function [23, Eqs. (1.2)-(1.3)].

*Proof:* The proof of Proposition 1 is provided in Appendix A. ■

By setting  $r = 1$ , it is noteworthy that the Fox's  $H$ -function in (13) can be reduced to the Meijer's  $G$ -Function [23, Eqs. (1.111), (1.112)] as

$$H_{0,2}^{2,0} \left( \epsilon(y) \left| \begin{matrix} -; - \\ (x, 1), (j, \frac{1}{r}); - \end{matrix} \right. \right) = G_{0,2}^{2,0} \left( \epsilon(y) \left| \begin{matrix} -; - \\ x, j; - \end{matrix} \right. \right), \quad (15)$$

where the couple  $(x, y)$  denotes either  $(1, \lambda)$  or  $(\alpha, \beta)$ .

Even though (13) is expressed in terms of non-elementary functions, it can be easily implemented using built-in Meijer's  $G$ -function in Matlab, or by the Fox's  $H$ -function implementation in Matlab [24].

#### IV. SECRECY ANALYSIS

In this Section, the intercept probability (IP) of the considered RF/UOWC system is derived. IP is defined as the probability that the capacity of the main link (i.e.,  $S - R - D$  link) is less than that of the wiretap link. In this case, the eavesdropper most likely succeeds to intercept the legitimate message. Mathematically speaking, IP corresponds to zero-secrecy rate event probability, being expressed as

$$P_{int} = \Pr(C_R < C_E), \quad (16)$$

where

$$C_R = \log_2(1 + \gamma_{eq}), \quad (17)$$

and  $C_E$  denote, the channel capacities of the  $S - R - D$  and  $S - E$  links, respectively.

We consider a scenario composed by  $L$  independent and non-coordinating eavesdroppers. The eavesdroppers aim to intercept independently the transmitted signal from  $S$  via an RF link. Consequently, the overall capacity of the wiretap channel from  $S$  to  $E$  is the maximum of the achievable individual capacities by the  $L$  eavesdroppers, i.e.,

$$C_E = \max_{i=1, \dots, L} (C_{SE_i}), \quad (18)$$

where  $C_{SE_i}$  denotes the  $S - E_i$  link capacity.

Since the maximum of the individual capacities  $(C_{SE_i})_{1 \leq i \leq L}$  corresponds to the maximum SNR of the links  $S - E_i$ , we have that

$$\gamma_{SE} = \max_{i=1, \dots, L} (\gamma_{SE_i}). \quad (19)$$

From above, the CDF of the overall wiretap link's SNR  $\gamma_{SE}$  can be expressed as

$$\begin{aligned} F_{\gamma_{SE}}(z) &= \Pr \left[ \max_{i=1, \dots, L} (\gamma_{SE_i}) < z \right] \\ &= \left( \frac{\gamma_{inc}(m_e, \sigma_e z)}{\Gamma(m_e)} \right)^L. \end{aligned} \quad (20)$$

By plugging (17) and (18) into (16), and by making some algebraic manipulations, we get

$$\begin{aligned} P_{int} &= \Pr(\gamma_{eq} < \gamma_{SE} | \gamma_{SE}) \\ &= \int_0^\infty F_{\gamma_{eq}}(z) f_{\gamma_{SE}}(z) dz, \end{aligned} \quad (21)$$

with  $f_{\gamma_{SE}}(z)$  being the PDF of the overall wiretap link, obtained by differentiating (20) with respect to  $z$  as

$$f_{\gamma_{SE}}(z) = \frac{L \sigma_e^{m_e}}{\Gamma^L(m_e)} [\gamma_{inc}(m_e, \sigma_e z)]^{L-1} e^{-\sigma_e z} z^{m_e-1}. \quad (22)$$

**Proposition 2.** *The IP of the considered mixed RF/UOWC system is given by*

$$\begin{aligned} P_{int} &= 1 - \sum_{v_1=0}^{L-1} \binom{L-1}{v_1} (-1)^{v_1} \sum_{m_e, v_1} \sigma_e^{\theta+m_e} \sum_{l=0}^{m N_r-1} \frac{1}{l!} \\ &\times \sum_{j=0}^l \binom{l}{j} \sigma^{l-j} (\delta + \sigma_e)^{j-l-\theta-m_e} (P_1 + P_2) \end{aligned} \quad (23)$$

with

$$P_1 = \frac{L \omega}{r \Gamma(m_e)} Z(1, \lambda) \quad (24)$$

$$P_2 = \frac{L(1-\omega)}{r \Gamma(\alpha) \Gamma(m_e)} Z(\alpha, \beta) \quad (25)$$

$$Z(x, y) = H_{1,2}^{2,1} \left( \xi(y) \left| \begin{matrix} (1+j-l-m_e-\theta, 1/r); - \\ (x, 1), (j, \frac{1}{r}); - \end{matrix} \right. \right) \quad (26)$$

where  $\xi(y) = \frac{\Delta}{y(\delta + \sigma_e)^{\frac{1}{r}}}$ ,  $\theta = \sum_{k=0}^{m_e-1} k(v_{k+1} - v_{k+2})$ ,  $\sum_{m_e, v_1}$  denotes  $\sum_{v_2=0}^{v_1} \sum_{v_3=0}^{v_2} \dots \sum_{v_{m_e}=0}^{v_{m_e-1}} \prod_{i=0}^{m_e-1} \binom{v_{i+1}}{v_{i+2}} \left( \frac{1}{i!} \right)^{v_{i+1}-v_{i+2}}$  with  $v_{m_e+1} = 0$ , and  $\delta = \sigma + v_1 \sigma_e$

*Proof:* The proof of Proposition 2 is provided in Appendix B. ■

#### V. ANALYTICAL AND SIMULATION RESULTS

In this section, some representative numerical examples are shown in order to examine the effects of the key system parameters on the overall performance of the considered mixed RF/UOWC system. Without loss of generality, the system channel parameters are set as  $m_e = 2$ ,  $\bar{\gamma}_e = \{0 \text{ dB}, 5 \text{ dB}, 10 \text{ dB}\}$ , and  $L = \{2, 3, 4, 5\}$  as the number of eavesdroppers for the wiretap link, while we set  $m = 1$  for the  $S - R$  hop fading severity, and  $\alpha = 6.7615$ ,  $\beta = 0.3059$ ,  $\lambda = 0.1992$ , and  $\omega = 0.5717$ , for the  $R - D$  link turbulence severity. We fix the relaying gain constant as  $C = 0.5$ . The proposed analysis is validated through Monte Carlo simulation.

In Fig. 1, the intercept probability metric is depicted as a function of average  $S - R$  link's average SNR per branch  $\bar{\gamma}$ . The curves are plotted for a fixed number of eavesdroppers  $L = 2$  and an average  $R - D$  SNR  $\mu_r = 3 \text{ dB}$ , with various values of relay's receive antennas  $N_r = \{2, 3\}$  and eavesdropper's average SNR  $\bar{\gamma}_e = \{0 \text{ dB}, 5 \text{ dB}\}$ , and using coherent technique ( $r = 1$ ). We can remark clearly from the figure that the analytical curves plotted from the expression (23) match with the simulation results in starred markers. Additionally, one can notice also from the curves the impact of the average SNR and the number of antennas on the secrecy performance. For instance, increasing  $\bar{\gamma}$ , which corresponds

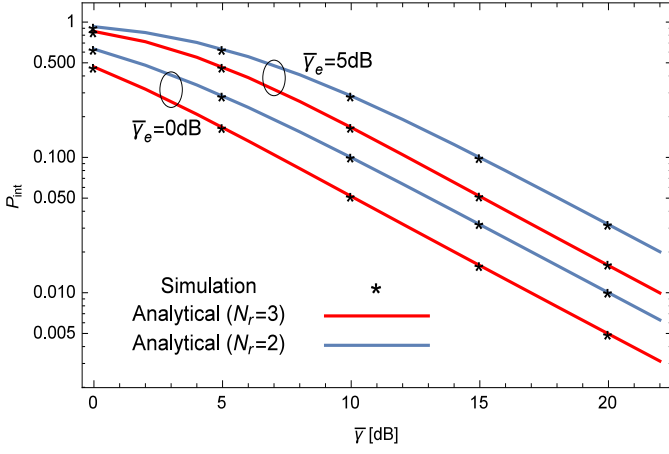


Fig. 1. Intercept probability versus average  $S - R$  SNR using coherent detection technique.

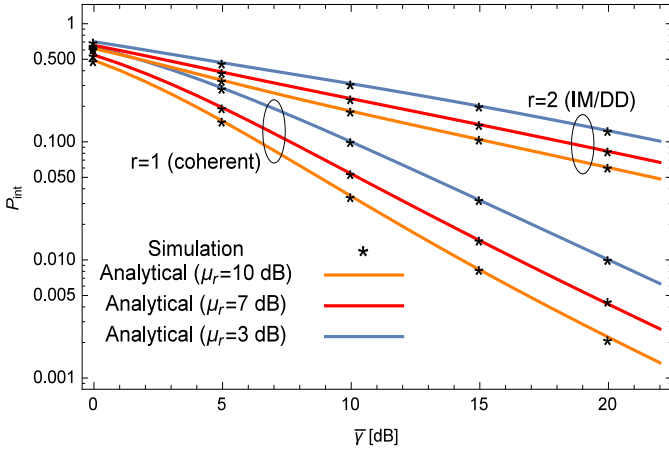


Fig. 2. Intercept probability versus average  $S - R$  SNR for various  $R - D$  SNR values.

to an increasing transmit power, or increasing the number of antennas yields a lower intercept probability and consequently achieving a better system's secrecy performance.

Fig. 2 shows the impact of the detection technique type as well as the  $R - D$  SNR  $\mu_r$  on the system secrecy performance. It can be clearly observed that coherent detection outperforms IM/DD in terms of system's secrecy performance. Moreover, the higher is the SNR  $\mu_r$  (i.e., higher relay transmit power or lower photodetector noise), the better is the achievable system's communication reliability.

In Fig. 3, the intercept probability is plotted as a function of the wiretap link average SNR  $\bar{\gamma}_e$ , for various values of eavesdropper nodes number and  $S - R$  average SNR (e.g.,  $L = 2, 3, 4$ ;  $\bar{\gamma} = 5 \text{ dB}, 15 \text{ dB}$ ). The  $R - D$  SNR was fixed as  $\mu_r = 3 \text{ dB}$  and we kept the fading and channel parameters values as for fig. 1. It is obviously seen from the curves that the intercept probability increases as a function of the wiretap channel's SNR, as well as the number of eavesdropping nodes. The more powerful is the wiretap link in terms of number of nodes (greater  $L$ ) and/or eavesdroppers received signal power,

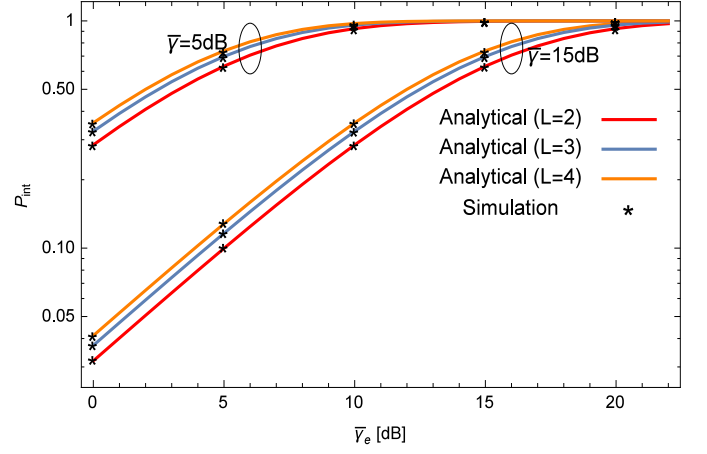


Fig. 3. Intercept probability versus average  $S - E$  SNR for various eavesdroppers number and using coherent detection technique.

the greater is the wiretap link capacity, and consequently, the more likely the legitimate communication is overheard. We can see additionally that the 3 curves' cluster on the right corresponding to a  $S - R$  SNR of 15 dB presents a better secrecy performance compared to the left curves (5 dB case), which confirms again that the higher is the transmit power, the more reliable is the communication.

## VI. CONCLUSION

In this work, we examined the secrecy performance of a dual-hop mixed RF/UOWC system. The considered system operates with a fixed-gain AF relaying scheme. An exact closed-form expression for the system's intercept probability metric is derived in terms of the Fox's  $H$ -function, and the impact of key system parameters on the overall secrecy performance was investigated.

A potential extension of this work is the consideration of multiple source nodes equipped with multiple antennas as well as taking into account the light beam pointing error impairment in the UOW link.

## APPENDIX A: PROOF OF PROPOSITION 1

By replacing the total end-to-end SNR by its expression given in (12), it yields

$$\begin{aligned} F_{\gamma_{eq}}(t) &= \Pr \left[ \frac{\gamma_{SR}\gamma_{RD}}{\gamma_{RD} + C} < t \right] \\ &= F_{\gamma_{SR}} \left( t \left( 1 + \frac{C}{z} \right) \middle| z \right) \\ &= \int_0^\infty F_{\gamma_{SR}} \left( t \left( 1 + \frac{C}{z} \right) \right) f_{\gamma_{RD}}(z) dz. \end{aligned} \quad (27)$$

By involving the expression of  $F_{\gamma_{SR}}(\cdot)$  and  $f_{\gamma_{RD}}(\cdot)$  given in (4) and (9), respectively, it yields

$$F_{\gamma_{eq}}(t) = B_1 + B_2, \quad (28)$$

with  $B_1$  and  $B_2$  being defined as

$$B_1 = \frac{\omega}{r\Gamma(mN_r)} \frac{\kappa}{\lambda} \int_0^\infty \gamma_{inc} \left( mN_r, \sigma t \left( 1 + \frac{C}{z} \right) \right) z^{\frac{1}{r}-1} \times \exp \left( -\frac{\kappa}{\lambda} z^{\frac{1}{r}} \right) dz, \quad (29)$$

$$B_2 = \frac{(1-\omega)}{r\Gamma(mN_r)\Gamma(\alpha)} \left( \frac{\kappa}{\beta} \right)^\alpha \int_0^\infty \gamma_{inc} \left( mN_r, \sigma t \left( 1 + \frac{C}{z} \right) \right) \times z^{\frac{\alpha}{r}-1} \exp \left( -\frac{\kappa}{\beta} z^{\frac{1}{r}} \right) dz. \quad (30)$$

Relying on the finite sum representation of the incomplete Gamma function [21, Eq. (8.352.1)],  $B_1$  can be rewritten as

$$B_1 = \omega \left( 1 - \frac{e^{-\sigma t}}{r} \sum_{l=0}^{mN_r-1} \frac{1}{l!} \sum_{j=0}^l (\sigma t)^{l-j} \binom{l}{j} \left( \frac{\sigma t C}{z} \right)^j \times \frac{\Delta}{(\sigma C)^{1/r} \lambda} \int_0^\infty e^{-\frac{\sigma t C}{z}} z^{\frac{1}{r}-1} \exp \left( -\frac{\Delta z^{\frac{1}{r}}}{(\sigma C)^{1/r} \lambda} \right) dz \right), \quad (31)$$

Now by applying the identities [25, Eq. (07.34.03.0228.01)], [25, Eq. (07.34.16.0002.01)], and [25, Eq. (07.34.21.0012.01)] we obtain

$$B_1 = \omega \left( 1 - \frac{e^{-\sigma t}}{r} \sum_{l=0}^{mN_r-1} \frac{1}{l!} \sum_{j=0}^l \binom{l}{j} (\sigma t)^{l-j} \times H_{0,2}^{2,0} \left( \frac{\Delta t^{1/r}}{\lambda} \middle| \begin{matrix} -; - \\ (1, 1), (j, 1/r); - \end{matrix} \right) \right), \quad (32)$$

The term  $B_2$  is computed in a similar manner. Hence it concludes the proof of Proposition 1.

## APPENDIX B: PROOF OF PROPOSITION 2

By involving the expressions of  $F_{\gamma_{eq}}(z)$  and  $f_{\gamma_{SE}}(z)$  from (13) and (22) into the IP formula (21), we obtain

$$P_{int} = 1 - \omega W(1, \lambda) - \frac{(1-\omega)}{\Gamma(\alpha)} W(\alpha, \beta), \quad (33)$$

with

$$W(x, y) = \frac{L}{r\Gamma^L(m_e)} \sum_{l=0}^{mN_r-1} \frac{1}{l!} \sum_{j=0}^l \binom{l}{j} \sigma^{l-j} \sigma_e^{m_e} \times \int_0^\infty [\gamma_{inc}(m_e, \sigma_e z)]^{L-1} e^{-z(\sigma_e + \sigma)} z^{l+m_e-j-1} \times H_{0,2}^{2,0} \left( \frac{\Delta z^{\frac{1}{r}}}{y} \middle| \begin{matrix} -; - \\ (x, 1), (1, 1/r); - \end{matrix} \right) dz. \quad (34)$$

Making use of the formula [21, Eq. (8.352.1)] alongside with the multinomial theorem, the term  $[\gamma_{inc}(m_e, \sigma_e z)]^{L-1}$  in the above equation can be written as

$$[\gamma_{inc}(m_e, \sigma_e z)]^{L-1} = (\Gamma(m_e))^{L-1} \sum_{v_1=0}^{L-1} \binom{L-1}{v_1} (-1)^{v_1} \times \sum_{m_e, v_1} (\sigma_e z)^\theta e^{-v_1 \sigma_e z}, \quad (35)$$

Involving (35) into (34), and by doing some algebraic manipulations, we get

$$W(x, y) = \frac{L}{r\Gamma(m_e)} \sum_{l=0}^{mN_r-1} \frac{1}{l!} \sum_{j=0}^l \binom{l}{j} \sigma^{l-j} \times \sum_{v_1=0}^{L-1} \binom{L-1}{v_1} (-1)^{v_1} \sum_{m_e, v_1} \sigma_e^{\theta+m_e} J(x, y), \quad (36)$$

with

$$J(x, y) = \int_0^\infty e^{-z(\delta + \sigma_e)} z^{l-j+m_e-1+\theta} \times H_{0,2}^{2,0} \left( \frac{\Delta z^{\frac{1}{r}}}{y} \middle| \begin{matrix} -; - \\ (x, 1), (j, 1/r); - \end{matrix} \right) dz. \quad (37)$$

By applying the formula [23, Eq. (2.19)] into the integral above, we obtain the result given in Proposition 2.

## REFERENCES

- [1] Z. Zeng, S. Fu, H. Zhang, Y. Dong, and J. Cheng, "A survey of underwater optical wireless communications," *IEEE Communications Surveys Tutorials*, vol. 19, no. 1, pp. 204–238, Firstquarter 2017.
- [2] E. Zedini, H. M. Oubei, A. Kammoun, M. Hamdi, B. S. Ooi, and M. S. Alouini, "A new simple model for underwater wireless optical channels in the presence of air bubbles," in *GLOBECOM 2017 - 2017 IEEE Global Communications Conference*, Dec 2017, pp. 1–6.
- [3] H. Kaushal and G. Kaddoum, "Underwater optical wireless communication," *IEEE Access*, vol. 4, pp. 1518–1547, 2016.
- [4] S. Arnon, J. Barry, G. Karagiannidis, R. Schober, and M. Uysal, *Advanced Optical Wireless Communication Systems*. The Edinburgh Building, Cambridge CB2 8RU, UK: Cambridge University Press, 2012.
- [5] M. V. Jamali, P. Khorramshahi, A. Tashakori, A. Chizari, S. Shahsavari, S. AbdollahRamezani, M. Fazelian, S. Bahrani, and J. A. Salehi, "Statistical distribution of intensity fluctuations for underwater wireless optical channels in the presence of air bubbles," in *2016 Iran Workshop on Communication and Information Theory (IWCIT)*, May 2016, pp. 1–6.
- [6] W. Liu, Z. Xu, and L. Yang, "SIMO detection schemes for underwater optical wireless communication under turbulence," *Photonics Research*, vol. 3, no. 3, pp. 48–53, June 2015.
- [7] I. S. Ansari, "On the performance of free-space optical systems over generalized atmospheric turbulence channels with pointing errors," February 2015.
- [8] E. Zedini, I. S. Ansari, and M. S. Alouini, "Performance analysis of mixed nakagami- $m$  and gamma-gamma dual-hop FSO transmission systems," *IEEE Photonics Journal*, vol. 7, no. 1, pp. 1–20, Feb 2015.
- [9] I. S. Ansari, F. Yilmaz, and M.-S. Alouini, "Performance analysis of free-space optical links over Málaga- $\mathcal{M}$  turbulence channels with pointing errors," *IEEE Transactions on Wireless Communications*, vol. 15, no. 1, pp. 91–102, January 2016.
- [10] M. Bloch, J. Barros, M. R. D. Rodrigues, and S. W. McLaughlin, "Wireless information-theoretic security," *IEEE Transactions on Information Theory*, vol. 54, no. 6, pp. 2515–2534, June 2008.

- [11] Y. R. Ortega, P. K. Upadhyay, D. B. da Costa, P. S. Bithas, A. G. Kanatas, U. S. Dias, and R. T. de Sousa Junior, "Joint effect of jamming and noise in wiretap channels with multiple antennas," in *2017 13th International Wireless Communications and Mobile Computing Conference (IWCMC)*, June 2017, pp. 1344–1349.
- [12] A. D. Wyner, "The wire-tap channel," *The Bell System Technical Journal*, vol. 54, no. 8, pp. 1355–1387, Oct 1975.
- [13] L. Wang, M. ElKashlan, J. Huang, R. Schober, and R. K. Mallik, "Secure transmission with antenna selection in MIMO Nakagami- $m$  fading channels," *IEEE Transactions on Wireless Communications*, vol. 13, no. 11, pp. 6054–6067, Nov 2014.
- [14] Y. Jiang, J. Zhu, and Y. Zou, "Secrecy outage analysis of multi-user cellular networks in the face of cochannel interference," in *2015 IEEE 14th International Conference on Cognitive Informatics Cognitive Computing (ICCI\*CC)*, July 2015, pp. 441–446.
- [15] F. J. Lopez-Martinez, G. Gomez, and J. M. Garrido-Balsells, "Physical-layer security in free-space optical communications," *IEEE Photonics Journal*, vol. 7, no. 2, pp. 1–14, April 2015.
- [16] X. Sun and I. B. Djordjevic, "Physical-layer security in orbital angular momentum multiplexing free-space optical communications," *IEEE Photonics Journal*, vol. 8, no. 1, pp. 1–10, Feb 2016.
- [17] H. Lei, Z. Dai, I. S. Ansari, K. H. Park, G. Pan, and M. S. Alouini, "On secrecy performance of mixed RF-FSO systems," *IEEE Photonics Journal*, vol. 9, no. 4, pp. 1–14, Aug 2017.
- [18] A. H. A. El-Malek, A. M. Salhab, S. A. Zummo, and M. S. Alouini, "Enhancing physical layer security of multiuser SIMO mixed RF/FSO relay networks with multi-eavesdroppers," in *2016 IEEE Globecom Workshops (GC Wkshps)*, Dec 2016, pp. 1–7.
- [19] M.-K. Simon and M.-S. Alouini, *Digital Communication Over Fading Channels*. New York: John Wiley and Sons, 2005.
- [20] Z. Chen, Z. Chi, Y. Li, and B. Vucetic, "Error performance of maximal-ratio combining with transmit antenna selection in flat Nakagami- $m$  fading channels," *IEEE Transactions on Wireless Communications*, vol. 8, no. 1, pp. 424–431, Jan 2009.
- [21] I. S. Gradshteyn and I. M. Ryzhik, *Table of Integrals, Series, and Products: Seventh Edition*. Burlington, MA: Elsevier, 2007.
- [22] M. O. Hasna and M. S. Alouini, "A performance study of dual-hop transmissions with fixed gain relays," *IEEE Transactions on Wireless Communications*, vol. 3, no. 6, pp. 1963–1968, Nov 2004.
- [23] A. Mathai, R. K. Saxena, and H. J. Haubol, *The H-Function Theory and Applications*. New York: Springer, 2010.
- [24] E. Illi, F. E. Bouanani, and F. Ayoub, "A performance study of a hybrid 5G RF/FSO transmission system," in *2017 International Conference on Wireless Networks and Mobile Communications (WINCOM)*, Nov 2017, pp. 1–7.
- [25] I. W. Research, *Mathematica Edition: version 11.3*. Champaign, Illinois: Wolfram Research, Inc., 2018.